Zeitschrift für Kristallographie 168, 197–212 (1984)

The rhombohedral structure of tricalcium silicate at 1200 °C

Fumito Nishi and Yoshio Takéuchi

Mineralogical Institute, Faculty of Science,
University of Tokyo, Hongo, Tokyo 113, Japan

Received: April 2, 1984

Crystal structure / Phase transition / Tricalcium silicate

Abstract. Crystals of tricalcium silicate having a monoclinic superstructure transformed into a rhombohedral structure when they were heated at 1200 °C with gas flame: $a=7.135(6)$ Å, $c=25.586(15)$ Å, space group $R3m$, and contents of $9\times Ca_{2.98}Si_{0.98}Al_{0.04}O_5$. The rhombohedral structure has been determined based on a set of 371 diffraction intensities measured with a single-crystal diffractometer giving a final value of $R=10\%$ for 159 reflections used.

The structure obtained is similar to the reported rhombohedral average structure of the monoclinic phase, but it has the following significant differences: (i) of the three independent silicate tetrahedra in the threefold axis, the orientation of the one about Si(1) is rotated by 60°, about the threefold axis, compared to that of the corresponding tetrahedron in the latter. (ii) The tetrahedron about Si(2) statistically points into opposite c directions, the fraction of the tetrahedron that points into one c direction being 70%, and (iii) all tetrahedra are tilted in such a way that their apical bonds, otherwise on the threefold axes, slightly swing away from the threefold axes with Si's being kept in the threefold axes.

The structural relationship is discussed between the rhombohedral and the triclinic phases.

Introduction

Tricalcium silicate is a well known compound exhibiting quite a few polymorphs. There are three triclinic phases up to 980 °C at which temperature this material is inverted to a monoclinic phase M1 (Bigaré, Guinier, Mazières, Regourd, Yannaquis, Eysel, Hahn and Woermann, 1967). This monoclinic phase is inverted to another monoclinic phase

M2 at 990 °C and then finally to a rhombohedral phase at 1050 °C (Bigaré et al., 1967). Although the existence of the two monoclinic phases may be recognized by minor differences in powder diffraction patterns, and by a small difference in differential thermal analysis, they are optically indistinguishable (Maki and Chromý, 1978). According to Maki (1978, 1982), there is a third monoclinic phase M3 between M2 and the rhombohedral phase. The rhombohedral phase is not quenchable but the monoclinic phase may in general be stabilized to room temperature by doping oxides such as MgO, Al_2O_3 and some others (Bigaré et al., 1967). Among these polymorphs, the monoclinic phases are characteristic of having complicated superstructures. The solution of the superstructures is thought to be of particular importance to elucidate the structural mechanism of the stepwise inversion in tricalcium silicate.

Golovastikov, Matveeva and Belov (1975) proposed the structure of the low-temperature triclinic phase, while Jeffery (1952) studied the pseudo-rhombohedral average structure of the monoclinic phase based on only the reflections of its average structure. Since the knowledge on the basic structure of the rhombohedral phase is of fundamental importance, we have undertaken a study of the structure at high temperatures anticipating that the result would throw light to unlabelling the long standing question on the superstructure of the monoclinic intermediate phases.

Experimental

Crystals of the Al_2O_3-stabilized M1 phase were used for the present study. They are platy with a maximum dimension of around 2 mm. Electron microprobe analyses yielded a chemical composition which may well be expressed by $Ca_{2.98}Si_{0.98}Al_{0.04}O_5$. Precession photographs revealed that they were unexceptionally twinned on the submicroscopic scale. The twinning domains are related to each other by 120° rotations around the pseudohexagonal c axis which is perpendicular to the plate. Using graphite monochromatized Mo$K\alpha$ radiation ($\lambda = 0.71069$ Å), we determined the cell dimensions from the 2θ values of 15 reflections measured with a four-circle single crystal diffractometer, Syntex $P2_1$; they are $a = 33.083(8)$ Å, $b = 7.027(2)$ Å, $c = 18.499(4)$ Å and $\beta = 94.12(2)°$. Those of the pseudo-rhombohedral average structure were then calculated as $a = 7.027$ Å, $c = 24.93$ Å.

With the use of a gas-flame heater and its temperature control system developed by Yamanaka, Takéuchi and Sadanaga (1981), precession photographs of the monoclinic crystals were taken at temperatures above the reported temperature for the monoclinic to rhombohedral inversion (Bigaré et al., 1967). In Fig. 1, a precession photograph showing $h0l$ reflections of the monoclinic phase at room temperature is compared with that at 1200 $\pm$ 50 °C. In this figure, we observe that the superstructure reflections of the

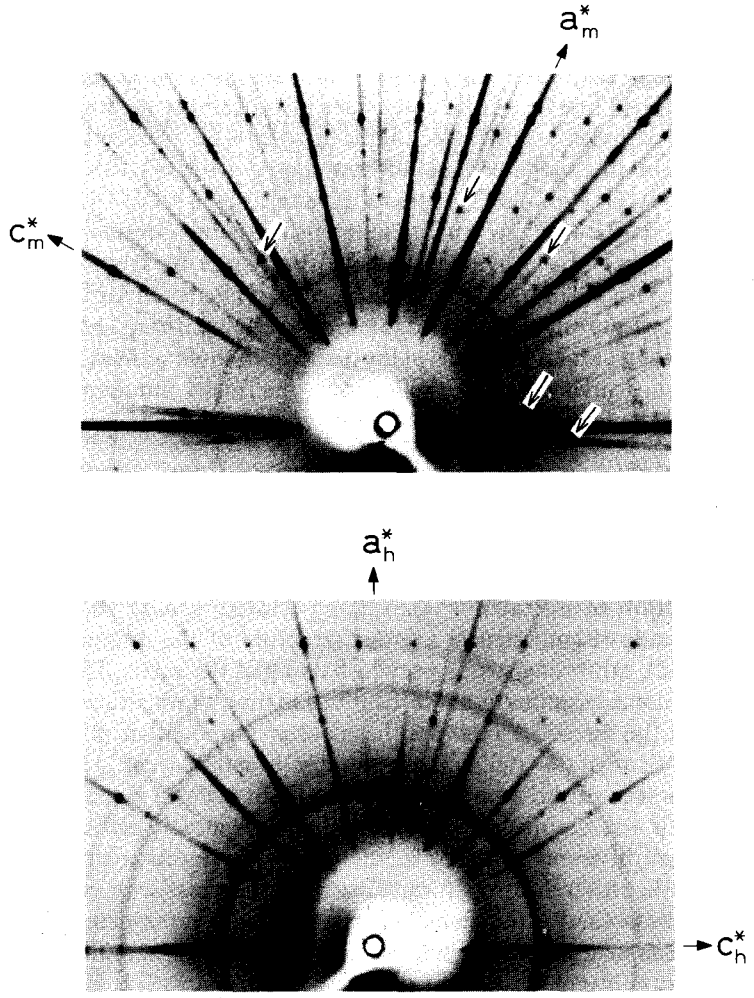

Fig. 1. Precession photographs showing $h0l$ reflections at room temperature (*top*) and at 1200 °C (*bottom*) (Mo$K\alpha$). Some of the superstructure reflections (*top*) are indicated by arrows, a^*_m and c^*_m indicating the reciprocal axes of the monoclinic cell and a^*_h and c^*_h those of the hexagonal cell of the rhombohedral phase. The powder diffraction patterns from zirconia cement are superposed in the photographs

former are completely missing in the latter. Taking into account the Laue photograph and the systematic absences of reflections, we confirmed that the high temperature phase was rhombohedral with possible space groups $R3m$, $R\bar{3}m$ or $R32$. For the above high-temperature experiments, crystals were directly put in the gas flame. We then noted that crystals showed a severe sublimation particularly at temperatures above 1300 °C.

Making allowance for such an effect of sublimation, we therefore selected a relatively large crystal piece having dimensions of $0.45 \times 0.4 \times 0.3$ mm for intensity study. Using the single-crystal diffractometer and the gas-flame heater mentioned above, Mo$K\alpha$ intensities of reflections were measured at 1200 ± 50 °C with the ω-2θ scan technique up to $2\theta = 60°$. The cell dimensions obtained from the single-crystal diffractometry are $a = 7.135(6)$ Å and $c = 25.586(15)$ Å. Of a total of 371 measured intensities, a set of 159 reflections were used for structural analysis, those intensities being omitted which were smaller than $3\sigma(I)$ and obviously affected by scattering from the cement materials used for mounting the crystal. They were corrected for Lorentz and polarization effects and for volume loss due to sublimation. The correction for volume loss was made in terms of the decrease in three standard intensities which were measured every fifty reflections; the final volume of the crystal was found to be 0.70 times initial volume.

Determination of the structure

Preliminary study

The distribution of diffraction intensities is closely similar to that of the reported pseudo-rhombohedral average structure of the monoclinic phase (Jeffery, 1952), exhibiting strong pseudo-halving of the a axis. This situation and packing considerations limit the locations of nine tetrahedra per cell to the positions on the threefold axes and the space group to either $R3m$ or $R\bar{3}m$.

A comparison of the triclinic structure (Golovastikov et al., 1975) and the average structure of the monoclinic phase (Jeffery, 1952) revealed that the location of Si and Ca atoms in both structures are closely similar. The two structures are different primarily in the relative orientation of the silicate tetrahedra; the difference might be caused by the change in coordination polyhedra about Ca due to thermal effects. The problem of determining the rhombohedral structure may then be reduced to the determination of the relative orientations of tetrahedra, the location of Ca and Si being nearly the same as that of the above-mentioned structures.

In the case of the noncentric space group $R3m$, Jeffery (1952) pointed out that there were eight possible rhombohedral structures in regard to the relative orientation of the silicate tetrahedra. Therefore, structure determination was started by refining the eight models using the least-squares program ORFLS (Busing, Martin and Levy, 1962). Throughout the present study, we used non-ionized atomic form factors (Vol. III of the *International Tables for X-ray Crystallography*, 1962), and applied unit weight for the least-squares calculations. Refinements of the eight models with anisotropic temperature factors gave values of R ranging from 10.2% to 19.0%. The results revealed that all models gave unusual Si–O bond lengths such as 1.17 Å or 1.91 Å, and very large B_{eq} values like 30 Å^2 or 65 Å^2. One of the

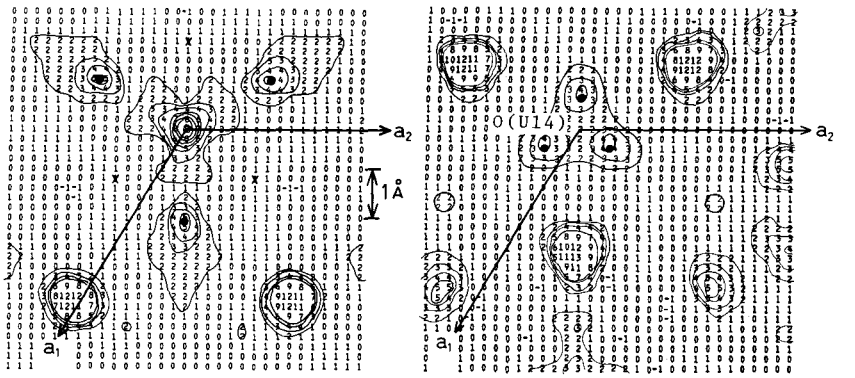

Fig. 2. (i) The Fourier section, $z = -0.025$, passing through basal oxygen atoms (small dots) of the Si(1) tetrahedron. The crosses indicate the locations of the corresponding oxygen atoms in the Jeffery model (Jeffery, 1952). (ii) The Fourier section, $z = 0.075$, showing that the Fourier peak corresponding to the apical oxygen atom, O(U14), is split into three maxima as indicated by small dots. In both sections, contours are drawn at an interval 0.5 eÅ^{-3} starting from one electron contour (figures have been multiplied by two). Heavy peaks are those of the Ca atoms not locating in the sections, their central contours being omitted

structures, which we designated 'Model 3', however, gave a relatively small number of unusual Si – O bond lengths and small values of B_{eq} compared to other models, the model giving an $R = 10.2\%$.

In the case of centric space group $R\bar{3}m$, we note that there are four possible structure models with regard to the relative orientation of the tetrahedra. In each case, one of the two distinct tetrahedra is located at the centers of symmetry; a split model is necessarily applied to that tetrahedron. Least-squares refinement of the four structures yielded R-values ranging from 10.4% to 20.0%. Resulting Si – O bond lengths and B_{eq}'s were even worse than those of the above noncentric models.

Fourier synthesis

We calculated structure factors using the coordinates of Ca, Si and the free oxygen atoms (the oxygen atoms not associated with Si), which were reported for the pseudorhombohedral average structure of the monoclinic phase (Jeffery, 1952), those of the oxygen atoms associated with tetrahedra being omitted. Then using the resulting phase angles, we made a Fourier synthesis of the rhombohedral phase. The Fourier map (Fig. 2) showed up the oxygen atoms of the silicate tetrahedra at the locations that support the structure of Model 3. The Fourier map, however, revealed a salient feature that the peaks showing the apical oxygen atoms on the

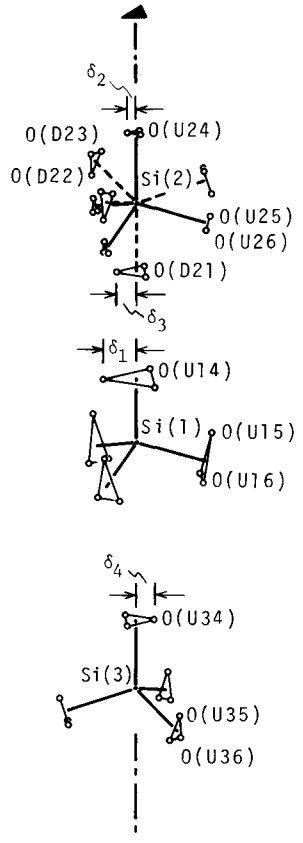

Fig. 3. Three independent tetrahedra on the threefold axis: Si(1) coordinated by O(U14), O(U15) and O(U16); Si(2) by O(D21), O(D22), O(D23), O(U24), O(U25) and O(U26); Si(3) by O(U34), O(U35) and O(U36)

threefold axes, in particular, are extending as shown in Fig. 2, suggesting that they are not exactly on the threefold axes but statistically distributed at positions off the threefold axes. The Fourier map further revealed that the Si(2) tetrahedron partly points into the *c* direction opposite to the one initially assumed.

These situations hinder the straightforward refinement of the structure. The major problem is now to estimate the displacements of the apical oxygen atoms from the threefold axes in Model 3, the displacement being denoted δ_1, δ_2, δ_3 and δ_4 for O(U14), O(U24), O(D21) and O(U34) respectively (Fig. 3). Note that in that figure each oxygen atom of the silicate tetrahedra is denoted by a set of two figures preceded by U or D. The first figure corresponds to the

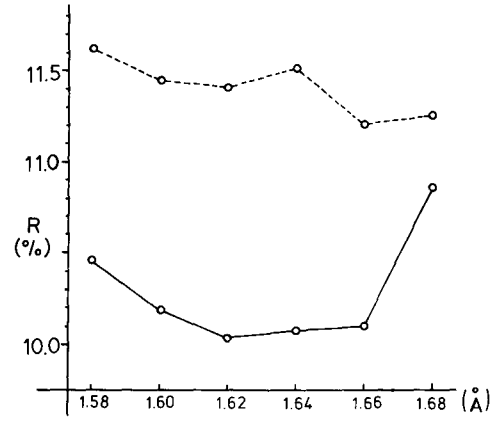

Fig. 4. A plot of R versus Si – O bond length for assumed regular tetrahedron formed by oxygen atoms about Si, the solid lines showing the case of the present structure model and broken lines that of the Jeffery model

notation of the Si atom to which the oxygen atom is bonded, the symbol U or D specifying whether the tetrahedron points up the c axis (U orientation) or points down (D orientation).

In order to estimate δ's, we first assumed that each tetrahedron has the shape of a regular tetrahedron with a fixed bond length of 1.62 Å. Then we refined the structure assuming various sets of fixed values of δ's; the parameters varied in each cycle were positional parameters and β_{ij}'s for Ca's, the z parameters and β_{ij}'s for Si's the z parameters for free O's, and isotropic temperature factors for all the oxygen atoms. As an initial step, least-squares calculations were made for various fixed values of δ_1, the remaining δ's being kept fixed to 0.4 Å; the R-value showed the lowest value of 10.25% for $\delta_1 = 0.7$ Å. Then a procedure similar to the above yielded $\delta_2 = 0.2$ Å; in this case δ_1 was fixed to the above value and both δ_3 and δ_4 to 0.4 Å. A number of repetition of such a procedure finally gave a set of values, $\delta_1 = 0.7$ Å, $\delta_2 = 0.2$ Å, $\delta_3 = 0.4$ Å and $\delta_4 = 0.4$ Å, which gave a lowest value of $R = 10.08$ %.

Finally with those values being fixed, refinements were made for various fixed values of the tetrahedral bond length other than 1.62 Å, the result showing that the value 1.62 Å was acceptable to a good approximation (Fig. 4). We observe in Fig. 4 that the difference in R is significant between Model 3 and other models including Jeffery's model for the average structure of the monoclinic phase. We may thus decide that Model 3 having the above values of δ well represents the rhombohedral structure at 1200 °C. The atomic coordinates and thermal parameters are listed in Table 1.

Table 1. Atomic parameters for tricalcium silicate at 1200 °C. (Values of the positional parameters are multiplied by 10^3)

Atomic notation	Occupancy	x	y	z	B_{eq}	B_{iso}
Ca(1)	1.0	488(1)	−488(1)	−001(2)	5.8 Å^2	
Ca(2)	1.0	826(2)	−826(2)	111(2)	7.3	
Ca(3)	1.0	509(1)	−509(1)	225(2)	4.0	
Si(1)	1.0	0	0	0	2.4	
Si(2)	1.0	0	0	213(2)	5.5	
Si(3)	1.0	0	0	784(2)	3.0	
O1	1.0	0	0	385(3)		3(1) Å^2
O2	1.0	0	0	504(9)		13(4)
O3	1.0	0	0	627(3)		1(1)
U14	1/3	057	−057	057		36(25)
U15	1/3	−130	130	007		11(4)
U16	1/3	223	148	−032		11(4)
U24	0.10(2)	016	−016	276		1(2)
U25	0.10(2)	−128	128	199		1(1)
U26	0.10(2)	241	130	188		1(1)
D21	0.23(2)	032	−032	152		1(2)
D22	0.23(2)	−131	131	219		1(1)
D23	0.23(2)	234	137	241		1(1)
U34	1/3	−032	032	845		5(4)
U35	1/3	131	−131	778		22(7)
U36	1/3	137	234	756		22(7)

Anisotropic thermal parameters ($\times 10^4$)

	β_{11}	β_{22}	β_{33}	β_{12}	β_{13}	β_{23}
Ca(1)	0301(41)	0301(41)	0033(3)	0175(55)	−0010(7)	0010(7)
Ca(2)	0244(53)	0244(53)	0050(7)	0062(64)	0014(9)	−0014(9)
Ca(3)	0277(49)	0277(49)	0015(2)	0165(59)	−0005(6)	0005(6)
Si(1)	0099(40)	0099(40)	0012(5)	0050(20)	0	0
Si(2)	0157(81)	0157(81)	0039(18)	0079(40)	0	0
Si(3)	0087(57)	0087(57)	0021(9)	0044(28)	0	0

Discussion

General features of the structure

The rhombohedral structure of tricalcium silicate thus brought out is illustrated in Fig. 5. The structure is as a whole similar to the pseudorhombohedral average structure of the monoclinic phase as proposed by Jeffery (1952); the three independent silicate tetrahedra are located on the threefold axes in the mirror plane and three independent calcium atoms likewise in the

Table 2. Valence sums at the oxygen atoms

Notation of oxygen atom	Bond valence (v.u.)			Σ
O1	Ca(1)	Ca(2)		
	0.277 × 3	0.306 × 3		1.748
O2	Ca(2)	Ca(3)		
	0.302 × 3	0.383 × 3		2.054
O3	Ca(1)	Ca(3)		
	0.502 × 3	0.264 × 3		2.297
U14	Ca(2)	Si(1)		
	0.311 × 3	1.000		1.934
U15 + U16	Ca(1)	Ca(3)	Si(1)	
	0.322 × 2	0.121 × 2	1.000	1.887
U24	Ca(1)	Si(2)		
	0.078 × 3	0.300		U24 + D21
D21	Ca(2)	Si(2)		= 1.972
	0.246 × 3	0.700		
U25 + U26	Ca(2)	Ca(3)	Si(2)	
	0.138	0.098 × 2	0.300	U25 + D22
D22 + D23	Ca(1)	Ca(3)	Si(2)	= 2.095
	0.191	0.285 × 2	0.700	
U34	Ca(3)	Si(3)		
	0.346 × 3	1.000		2.037
U35 + U36	Ca(1)	Ca(2)	Si(3)	
	0.310	0.347 × 2	1.000	2.004

set of mirror planes. There are however two major differences between the two.

Firstly, the silicate tetrahedra show an orientational disorder which may well be characterised by tiltings of the tetrahedra with the Si atoms being fixed on the threefold axis. As a result, each oxygen atom of the silicate tetrahedra is split into a set of three positions as shown in Fig. 5. In addition to those tiltings, a specific tetrahedron denoted Si(2) takes another mode of orientational disorder; a fraction in the amount of 70% of the tetrahedron points down the c axis, the remaining fraction pointing up the c axis.

Secondly, the Si(1) tetrahedron of the high-temperature structure is rotated by 60°, about the threefold axis, relatively to the corresponding tetrahedron of Jeffery's model. Because of such a difference, the sixfold coordination of Ca(3) in Jeffery's model is changed to sevenfold in the high-temperature structure. As a result, Pauling's electrostatic valence rule which is satisfied for Jeffery's model is apparently not exactly obeyed for the high-temperature structure. A trial was then made calculating the valence sum at

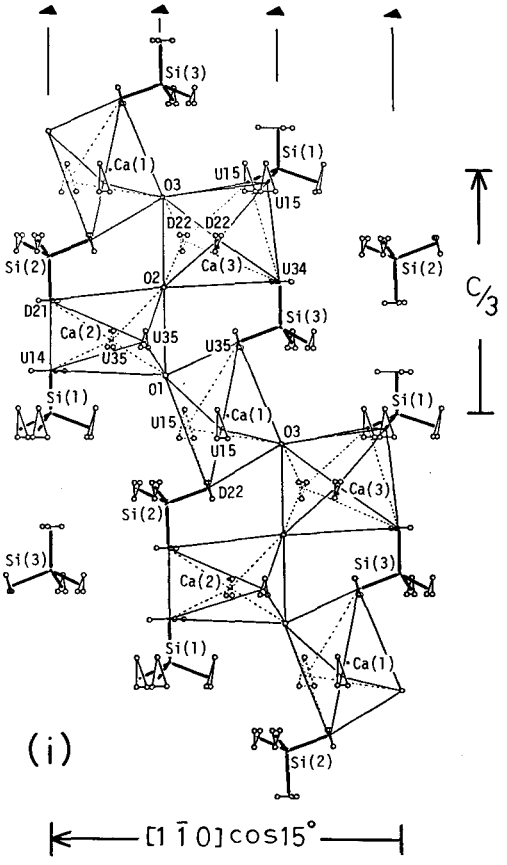

Fig. 5. The structure of the rhombohedral phase of tricalcium silicate at 1200 °C, showing the silicate tetrahedra and the polyhedra about the Ca atoms in the mirror plane parallel to (110) and passing through the origin. Because of the statistical orientation of the Si(2) tetrahedron, the structure is illustrated in two separate diagrams: (i) the case in which the Si(2) tetrahedron points down the *c* axis and (ii) the case in which it points up. They are views down [110] but rotated by 15° about the *c* axis. Each triangle indicates a triplet of split oxygen atoms but the atomic labellings of O(U16), O(U26), O(U36) and O(D23) are omitted

each oxygen atom following the procedure given by Donnay and Allmann (1970); for this calculation we used the statistical bond lengths as will be defined later. Table 2 gives the result. We observe valence sums in the range from 1.75 to 2.30 v.u. With the tolerance that the silicate groups were approximated as regular tetrahedra and that we used statistical bond lengths, we may decide that the resulting values are acceptable.

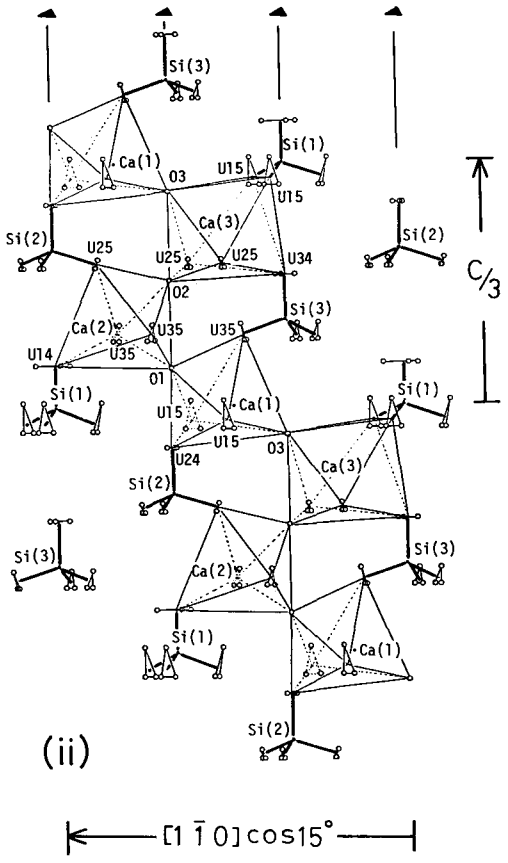

Fig. 5

Characteristics of the coordination polyhedra about Ca

With regard to split oxygen atoms, the Ca – O distances listed in Table 3 are divided into two categories: (1) Those between Ca and individual split positions, and (2) those between Ca and the positions at which the oxygen atoms would be located if the tiltings of the tetrahedron were disregarded and the Si – O bond length of 1.62 Å kept unchanged. Each oxygen position as defined in (2) may be regarded as an average position of a set of three split oxygen atoms. Thus the bonds in the second category may be called statistical bond lengths.

For both cases in which the Si(2) tetrahedron takes the U and D orientation, the polyhedra about Ca are constructed and compared in Fig. 5. As will be observed in this figure (and Table 3), Ca(1) and Ca(2) have sixfold

Table 3. Ca–O bond lengths

	Oxygen atom		Ca–O bond			Oxygen atom		Ca–O bond	
	Notation	Symmetry code	Multiplicity	Length		Notation	Symmetry code	Multiplicity	Length
Ca(1)	O3	vii m	1.0	2.15(4) Å	Ca(3)	U25	ii j	0.10	2.39(1) Å
	U36	ix m	1/3	2.36(5)		U25	iii k	0.10	2.39(1)
	U36	xi m	1/3	2.36(5)		O2	xiii m	1.0	2.39(14)
	U15	ii j	1/3	2.383(7)		U26	i k	0.10	2.50(2)
	U15	iii k	1/3	2.383(7)		U26	iv j	0.10	2.50(2)
	U16	i k	1/3	2.46(2)		D23	iii j	0.233	2.527(8)
	U16	iv j	1/3	2.46(2)		D23	v k	0.233	2.527(8)
	D23	xiv m	0.233	2.46(5)		U16	ix k	1/3	2.57(3)
	D23	xviii m	0.233	2.46(5)		U16	xi k	1/3	2.57(3)
	U24	xiv m	0.10	2.56(3)		U26	iii j	0.10	2.58(2)
	U24	xv m	0.10	2.56(3)		U26	v k	0.10	2.58(2)
	O1	xiii m	1.0	2.59(5)		O3	xiii m	1.0	2.63(6)
	U24	xiii m	0.10	2.81(3)		U34	vii m	1/3	2.83(2)
	U16	iii j	1/3	2.84(2)		U16	vii k	1/3	2.93(3)
	U16	v k	1/3	2.84(2)		U16	x k	1/3	2.93(3)
	U35	vii m	1/3	2.89(5)		U35	vii m	1/3	2.95(4)
	D22	xiii m	0.233	2.96(5)					
						Statistical bond lengths			
Ca(2)	U26	ii l	0.10	2.09(5)					
	U26	vi l	0.10	2.09(5)	Ca(1)	O3	vii m	1.0	2.15(4)
	D21	ii l	0.233	2.24(2)		U35	vii m	1.0	2.51(5)
	D21	iii l	0.233	2.24(2)		U15	ii j	1.0	2.48(1)
	U35	viii n	1/3	2.286(6)		U15	iii k	1.0	2.48(1)
	U35	ix p	1/3	2.286(6)		D22	xiii m	0.7	2.60(5)
	U25	i l	0.10	2.34(5)		U24	xiii m	0.3	2.63(3)
	U14	ii l	1/3	2.34(3)		O1	xiii m	1.0	2.59(5)
	U14	iii l	1/3	2.34(3)					

Ca(2)	U36	vii	n	1/3	2.37(1)	Ca(2)	U25	i	l	0.3	2.17(5)
	U36	x	p	1/3	2.37(1)		D21	i	l	0.7	2.37(2)
	O1	xiii	m	1.0	2.48(5)		U35	viii	n	1.0	2.38(1)
	O2	xiii	m	1.0	2.49(15)		U35	ix	p	1.0	2.38(1)
	U36	viii	p	1/3	2.56(1)		U14	i	l	1.0	2.47(3)
	U36	xii	n	1/3	2.56(1)		O1	xiii	m	1.0	2.48(5)
	U15	i	l	1/3	2.71(5)		O2	xiii	m	1.0	2.49(15)
	D21	i	l	0.233	2.75(2)						
	D22	i	l	0.233	2.82(5)	Ca(3)	D22	ii	j	0.7	2.350(6)
	U14	i	l	1/3	3.16(2)		D22	iii	k	0.7	2.350(6)
							U34	vii	m	1.0	2.45(2)
Ca(3)	D22	ii	j	0.233	2.283(5)		U25	ii	j	0.3	2.48(2)
	D22	iii	k	0.233	2.283(5)		U25	iii	k	0.3	2.48(2)
	U34	viii	m	1/3	2.33(2)		O2	xiii	m	1.0	2.39(14)
	U34	ix	m	1/3	2.33(2)		U15	viii	k	1.0	2.96(3)
	D23	i	k	0.233	2.335(8)		U15	ix	k	1.0	2.96(3)
	D23	iv	j	0.233	2.335(8)		O3	xiii	m	1.0	2.63(6)

Symmetry code

i	x, y, z	xiv	$2/3-y, 1/3+x-y, 2/3+z$
ii	$-y, x-y, z$	xv	$2/3-x+y, 1/3-x, 2/3+z$
iii	$-x+y, -x, z$	xvi	$2/3-y, 1/3-x, 2/3+z$
iv	$-y, -x, z$	xvii	$2/3+x, 1/3+x-y, 2/3+z$
v	$x, x-y, z$	xviii	$2/3-x+y, 1/3+y, 2/3+z$
vi	$-x+y, y, z$		
vii	$1/3+x, 2/3+y, 1/3+z$	j	+a
viii	$1/3-y, 2/3+x-y, 1/3+z$	k	−b
ix	$1/3-x+y, 2/3-x, 1/3+z$	l	+a−b
x	$1/3-y, 2/3-x, 1/3+z$	m	−b−c
xi	$1/3+x, 2/3+x-y, 1/3+z$	n	−2b−c
xii	$1/3-x+y, 2/3+y, 1/3+z$	p	+a−b−c
xiii	$2/3+x, 1/3+y, 2/3+z$		

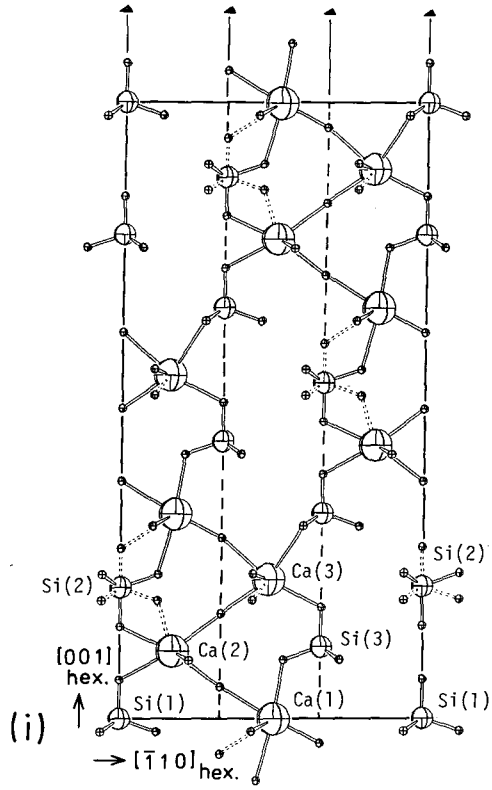

Fig. 6. Comparison of the structures of (i) the rhombohedral phase at 1200 °C and (ii) the triclinic phase (T1). The former is a view down [110] of the arrangement of the cations in the mirror plane as in Fig. 5 and the oxygen atoms associated with them, each triplet of split oxygen atoms (Fig. 5) being represented by a single oxygen atom at their statistical position (see text). The latter triclinic structure shows its atomic layer corresponding to the former, a view down [111]. The triclinic cell is indicated, the origin being in the layer of Ca atoms directly below the atomic layer illustrated

coordinations, while Ca(3) has a sevenfold coordination. In the case of the polyhedra about Ca(3), however, two of the seven bonds have a fairly longer value of 2.96 Å (category (2)) compared to others. The coordination of Ca(3) may then be regarded as basically fivefold. This situation is well in accord with the fact that the coordination number of a cation tends to be reduced with increasing temperature to provide more freedom for thermal vibration of the cation. An over-all average of the Ca – O bond lengths gives a value of 2.51 Å which is to be compared with the average value of 2.39 Å for the pseudorhombohedral average structure of the monoclinic phase (Jeffery, 1952); our value at 1200 °C is about 5.0% larger than Jeffery's value at room temperature.

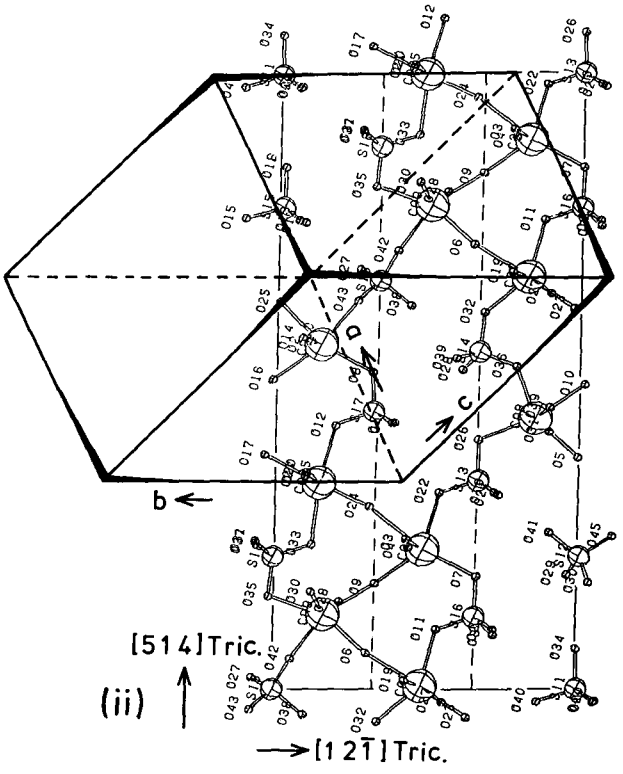

Fig. 6

Comparison with the triclinic structure

In Fig. 6, we compare the atomic arrangement of the rhombohedral structure with that of the low-temperature triclinic structure (Golovastikov et al., 1975). As will be observed in this figure, the major difference between the two is in the relative orientation of silicate tetrahedra, the positions of Ca, Si and free oxygen atoms being closely similar. In the triclinic structure, two of the twenty-nine independent Ca atoms are seven-coordinated with a maximum bond length of 2.704 Å and the remaining twenty-seven Ca atoms may be considered to have sixfold coordinations. Each of the five polyhedra about Ca atoms in the structure gives an average Ca−O bond length which is slightly longer than 2.45 Å, while the over-all mean of the Ca−O bond lengths in the remaining 24 polyhedra is 2.401 Å. This situation is to be compared with that of the present structure in which one of the three independent Ca atoms has basically fivefold coordination and the remaining

have sixfold coordination. It is then highly conceivable that stepwise decreasings of the number of seven- or six-coordinated Ca atoms (with increasing temperature) would basically characterize the complicated series of the phase transformations in tricalcium silicate. In order to study this problem we have fully determined the superstructure of the M1 phase and the structure of another monoclinic phase. The results will be reported later.

References

Bigaré, M., Guinier, A., Mazières, C., Regourd, M., Yannaquis, N., Eysel, W., Hahn, Th., Woermann, E.: Polymorphism of tricalcium silicate and its solid solutions. Am. Ceram. Soc. Bull. **50**, 609–619 (1967)

Busing, W. R., Martin, K. O., Levy, H. A.: ORFLS. Oak Ridge National Laboratory Report ORNL-TM-305 (1962)

Donnay, G., Allmann, R.: How to recognize O^{2-}, OH^- and H_2O in crystal structures determined by X-rays. Am. Mineral. **55**, 1003–1015 (1970)

Golovastikov, R., Matveeva, R. G., Belov, N. V.: Crystal structure of the tricalcium silicate $3CaO \cdot SiO_2 = C_3S$. Sov. Phys. Crystallogr. **20**, 441–445 (1975)

Jeffery, J. W.: The crystal structure of tricalcium silicate. Acta Crystallogr. **5**, 26–35 (1952)

Maki, I., Chromý, S.: Microscopic study on the polymorphism of Ca_3SiO_5. Cem. Concr. Res. **8**, 407–414 (1978)

Maki, I., Kato, K.: Phase identification of alite in Portland cement clinker. Cem. Concr. Res. **12**, 93–100 (1982)

Yamanaka, T., Takéuchi, Y., Sadanaga, R.: Gas-flame, high temperature apparatus for single-crystal X-ray diffraction studies. Z. Kristallogr. **154**, 147–153 (1981)